

Proper Motion of Pulsar B1800–21

W. F. Brisken

*National Radio Astronomy Observatory, P.O. Box O, Socorro, NM 87801;
wbrisken@nrao.edu*

M. Carrillo-Barragán¹ and S. Kurtz

Centro de Radioastronomía y Astrofísica, UNAM Morelia, Michocán, México

and

J. P. Finley

*Physics Department, Purdue University, 525 Northwestern Avenue West Lafayette, IN
47907-2036*

ABSTRACT

We report high angular resolution, multi-epoch radio observations of the young pulsar PSR B1800–21. Using two pairs of data sets, each pair spanning approximately a 10 year period, we calculate the proper motion of the pulsar. We obtain a proper motion of $\mu_\alpha = 11.6 \pm 1.8 \text{ mas yr}^{-1}$, $\mu_\delta = 14.8 \pm 2.3 \text{ mas yr}^{-1}$, which clearly indicates a birth position at the extreme edge of the W30 supernova remnant. Although this does not definitively rule out an association of W30 and PSR B1800–21, it does not support an association.

Subject headings: pulsars: individual(B1800–21) — supernovae: individual (W30)

1. Introduction

Pulsar-supernova remnant associations are important for various reasons. When an association is confirmed, knowledge of the supernova remnant (SNR) can be used to constrain

¹Instituto de Astronomía, UNAM, Apdo. Postal 70 - 264, Ciudad Universitaria, México, D.F., CP 04510

pulsar (PSR) parameters such as birth magnetic fields, spin periods, luminosities, and beaming fractions. Conversely, knowledge of the pulsar can constrain SNR ages and distances, and illuminate remnant evolution and uncommon morphologies (Kaspi 1996). Although over 30 candidate pulsar-SNR associations are purported, fewer than a dozen have been confirmed.

Although confirmation of an association is desirable, the opposite — disproving an association — can also be useful. Pulsar proper motions, which are often cited to support associations, can be a definitive means to disprove candidate associations. Even if an association is disproven, the pulsar transverse velocity is useful information. It can constrain stellar collapse models and contribute to studies of pulsar velocity distributions and galactic electron density distributions (e.g., Chatterjee et al. 2001).

2. PSR 1800–21 and SNR W30

PSR B1800–21 and SNR W30 have been the object of several studies, including Odegard (1986), Kassim & Weiler (1990), Frail et al. (1994), and Finley & Ögelman (1994). An association between the two has been actively discussed: Kassim & Weiler suggest a weak association based on similar age and position. Frail et al. argue that the association is unlikely, based on the absence of a pulsar wind nebula (owing to the high transverse velocity if the supernova occurred at the center of the remnant) and the discrepancy between OH and HI line profiles; and Finley & Ögelman present X-ray data and interpret the SNR morphology as an interaction with the ambient medium, which might salvage the association.

Pulsar B1800–21 was discovered by Clifton & Lyne (1986) in their high-radio-frequency survey for young and millisecond pulsars. It is bright ($S_{1400\text{MHz}} = 7.6$ mJy) ranking 70 of 1162 pulsars with known $S_{1400\text{MHz}}$ as per version 1.24 of the ATNF pulsar database (Manchester et al. 2005). It is also young, with a characteristic age $\tau_c \equiv P/2\dot{P} = 15.8$ kyr, ranking 31 of 1560 pulsars known to date (Manchester et al. 2005). It is well established that for many young pulsars the characteristic age is a poor indicator of true age. A non-zero spin period at birth would over-estimate the pulsar age, while a braking index smaller than the nominal value of 3 would under-estimate the age. Nevertheless, the characteristic age of B1800–21 is in rough agreement with the SNR age (15 – 28 kyr) under the assumption of a blast energy of 10^{51} ergs (Finley & Ögelman 1994). Adopting 15.8 kyr for both objects, and assuming that the supernova occurred at the geometric center of the remnant, the pulsar would need an extreme transverse velocity of ~ 1700 km s⁻¹ in the south-west direction to reach its present position.

The dispersion measure (DM) distance currently gives the best estimate of the pulsar’s

distance. The Taylor & Cordes (1993) Galactic electron density model yields 3.9 kpc for the pulsar’s $DM=233.99 \text{ pc cm}^{-3}$. The newer Cordes & Lazio NE2001 model (Cordes & Lazio 2002) yields a similar value of $3.84^{+0.39}_{-0.45} \text{ kpc}$.¹

W30 is a roughly spherical SNR, about $50'$ in diameter, with PSR B1800–21 lying to the south-west of the geometrical center (see Fig. 1). Kassim & Weiler (1990) suggested a distance of $6 \pm 1 \text{ kpc}$ to the SNR, based on association with HII regions. At this distance, the $50'$ size corresponds to 80 pc. Revised models of the galactic rotation curve (Brand & Blitz 1993) indicate that the HII regions, and by inference the SNR, are about 4.8 kpc distant. Finley & Ögelman (1994), assuming an initial blast energy of 10^{51} ergs, find a distance range of 3.2 – 4.3 kpc.

The 5.3 kpc distance originally reported for the pulsar (Clifton & Lyne 1986) was sufficiently close to the (then) $6 \pm 1 \text{ kpc}$ SNR distance to encourage the idea of an association. Refinements to the pulsar and the SNR distances have revised both distances downward, keeping hopes for an association alive. In particular, the $3.39^{+0.39}_{-0.45} \text{ kpc}$ distance estimate for the pulsar is in reasonable agreement with the 3.2 – 4.3 kpc distance estimate for the SNR.

With the goal of ascertaining the relative motion of the pulsar with respect to the SNR, we undertook a program to measure the pulsar proper motion. To date the only measurement of this proper motion is the nondetection of $\mu_\alpha = 18 \pm 30 \text{ mas yr}^{-1}$, $\mu_\delta = 400 \pm 470 \text{ mas yr}^{-1}$ by Zou et al. (2005) using pulsar timing.

3. Observations and Data Reduction

New observations of the pulsar were obtained with the NRAO² Very Large Array (VLA) on 2002 February 8 at 21 cm and on 2005 February 5 at 3.6 cm. Each of these observations of PSR B1800–21 was paired with a data set from the VLA archive observed in a similar mode. The 2002 (21 cm) data were taken in spectral line mode, and were paired with line data from program AV201 taken on 1993 January 18. The 2005 (3.6 cm) data were taken in continuum mode and were paired with continuum data from program AF244 taken on 1993 March 14. A summary of the observational parameters for each of the four data sets is provided in Table 1.

Each of the four data sets was calibrated and imaged individually (see §§3.1 and 3.2

¹All uncertainties reported reflect the most compact interval containing 68.3% of the probability.

²The National Radio Astronomy Observatory is a facility of the National Science Foundation operated under cooperative agreement by Associated Universities, Inc.

below). The two pairs of data sets (one of line data, the other of continuum) provide two independent estimates of the pulsar’s proper motion using independent techniques.

3.1. Continuum Data

The AF244 and AC774 3.6 cm observations of PSR B1800–21 were directly referenced to a standard VLA calibrator, B1748–253 or J1751-2524, allowing an absolute position determination.

Data reduction followed normal procedures, with several exceptions. The AF244 data were taken in B1950 coordinates while the AC774 data were taken in J2000.0 coordinates. To render the two data sets fully comparable we performed several additional operations on the AF244 data. First, when needed, the coordinates were transformed from B1950 to J2000.0 using the AIPS task UVFIX. Next, UVFIX was used a second time to correct for the UT1-UTC difference and to correct for a time-stamping error common to all VLA observations. Finally, the coordinates of the phase calibrator (B1748–253) were updated from their 1993 values to the improved position used for the 2005 observations (J1751–2524). We used the VLA calibrator manual³ J2000 position $17^h51^m51.263047^s -25^\circ24'00.060610''$ with an expected accuracy of < 10 mas.

AF244 observed the pulsar once during source rise and once during transit. As a third step, the source-rising scan was omitted in order to match the uv plane coverage more closely to that of the transit-only AC774 observation. The final image noise and resolution for both observing dates are given in Table 1.

3.2. Spectral Line Data

The AV201 and AC629 programs both observed at 21 cm in the A-configuration using 15 spectral channels spanning a 23.5 MHz band in two polarizations. Due to an apparent front-end filter misconfiguration during the AV201 observations, only spectral channels 8 through 14 were used; the remaining channels were highly attenuated. For the AC629 reduction, channels 2 through 14 were retained. Channels 1 and 15 were omitted because the bandpass was steeply sloped there, possibly introducing non-closing errors. Self-calibration was performed for both data sets.

³Available at <http://www.aoc.nrao.edu/~gtaylor/calib.html>

Wide-field imaging was used to image the pulsar and eight additional sources found within the primary beam. Five of these sources were point-like, and served to define a reference frame in which (following McGary et al. 2001) a precise proper motion could be determined. All nine sources detected are listed in Table 2.

4. Proper Motion Analysis

The two continuum data sets have a time baseline of 4346.08 days (11.90 yr). Given the positions listed in Table 3, we calculate proper motions in right ascension (α) and declination (δ) of $\mu_\alpha = 11.4 \pm 3.4$ mas yr $^{-1}$ and $\mu_\delta = 13.7 \pm 3.5$ mas yr $^{-1}$. The two spectral line data sets have a time baseline of 3317.84 days (9.08 yr). The source positions of these two observations imply proper motions of $\mu_\alpha = 11.7 \pm 2.2$ mas yr $^{-1}$ and $\mu_\delta = 15.7 \pm 3.1$ mas yr $^{-1}$.

For the continuum data, the uncertainty in the pulsar coordinates was determined by the measurement of the proper motion of an additional calibrator source, J1832–1035, which was observed during both epochs. Although a null result was expected, a non-zero result was obtained. This check source was 3.37 and 3.92 times more distant from the phase calibrator J1751–2524 than was the pulsar, in right ascension and declination, respectively. The uncertainty in each coordinate of the pulsar proper motion was derived from the observed proper motion of this check source divided by this factor. For the line data sets, the uncertainty in the pulsar coordinates is a statistical error from the coordinate system defined by the five point sources.

The agreement between the two independent proper motion estimates for the pulsar is reassuring, and suggests that a single, combined proper motion is warranted. The signal-to-noise ratio weighted combined proper motion is $\mu_\alpha = 11.6 \pm 1.8$ mas yr $^{-1}$ and $\mu_\delta = 14.8 \pm 2.3$ mas yr $^{-1}$. The total proper motion is thus $\mu_{\text{total}} = 18.7_{-1.5}^{+1.4}$ mas yr $^{-1}$ in the direction 38.1° east of north.

These 3.6 cm continuum observations offer the best measurement of the absolute position of the pulsar on the sky. The J2000.0 coordinates of the pulsar are determined to be $18^h03^m51.4105^s$, $-21^\circ37'07.351''$ at MJD 51544.0 (2000 January 1) with error of about 10 mas in each coordinate. Relevant parameters of the pulsar are listed in Table 3.

5. Discussion

The newly measured proper motion, together with an adopted distance, can be used to determine the transverse velocity of the pulsar. The NE2001 distance, $D = 3.8 \pm 0.4$ kpc,

was used to compute a transverse velocity of 347_{-48}^{+57} km s⁻¹. This calculation includes a correction of 0.64 mas yr⁻¹ for the combined effects of the Sun’s peculiar motion and the differential Galactic rotation. The net effect of this correction is that the LSR transverse speed is 8 km s⁻¹ greater than its apparent speed. This speed is well within the normal range of young pulsar speeds (see, e.g. Arzoumanian et al. 2002 and Brisken et al. 2003) which suggests that the DM distance estimate is reasonable.

Independently of the distance estimation, an assumed pulsar age, together with the measured apparent proper motion, allows the calculation of the pulsar birthplace coordinates. In particular, assuming 15.8 kyr for B1800–21, and a proper motion of $\mu_{\text{total}} = 18.7_{-1.5}^{+1.4}$ mas yr⁻¹ 38.1° east of north, its birthplace in J2000.0 is $\alpha_0 = 18^{\text{h}} 03^{\text{m}} 38.0^{\text{s}} \pm 2.3^{\text{s}}$, $\delta_0 = -21^{\circ} 41' 18.2'' \pm 41.6''$.

The characteristic age for the pulsar is based purely on the observed pulse period and its derivative and is a good proxy for the true age given two conditions: (1) spindown is due to the magnetic dipole radiation leading to braking index $n = 3$, and (2) the initial spin period was much less than the current spin period.

Livingstone et al. (2005) note that all braking index measurements made give values less than the nominal $n = 3$. Only very young pulsars have such measurements so it might be safe to assume that B1800–21 has $n < 3$. In fact, an index as low as 2 is reasonable, which would double its true age. If so, the birth site would be even further from the W30 remnant, and would nearly coincide with the HII region G8.14+0.23 (IRAS 17599–2148) and the dark cloud, traced by mid-IR emission (see Fig. 1). We note that this HII region is probably unrelated to the pulsar-SNR complex; radio recombination line velocities suggest that it is kinematically distinct from the other HII regions found near the remnant (Lockman 1989).

Faucher-Giguere & Kaspi (2006) have tabulated initial spin periods that have been estimated for nine young pulsars. Four have values less than or about 30 ms, four more are between 50 and 90 ms, and one exceptional case (PSR J0538+2817) is quite long, at 140 ms. Based solely on these values it seems unlikely that the true age is less than half the characteristic age. However, serious selection effects have likely biased this sample. Through population modeling Faucher-Giguere & Kaspi (2006) conclude that a wider range of birth spin periods is actually likely. Assuming a normally-distributed birth spin period, they report a distribution with $\mu = 300$ ms and $\sigma = 150$ ms. Given that the current spin period of B1800–21 is 134 ms, this distribution is clearly not useful in estimating P_0 for this pulsar. Thus the characteristic age is likely correct to a factor of 2; claiming an age range much smaller than this is not well-justified.

It is clear that the pulsar did *not* originate at the geometric center of W30, as seen in the Kassim & Weiler (1990) image. First, the birthplace coordinates are far-removed from the SNR center for any assumed age. Second, the pulsar is currently at a position approximately 106° west of north (in equatorial coordinates) with respect to the center of W30. The proper motion, at 38° east of north, is more nearly *toward* the center of W30, rather than away from it.

A more sensitive image of the W30 remnant has been reported by Brogan et al. (2006) (see Fig. 1). This image shows W30 to be the bright, eastern part of a larger, non-thermal nebula. Despite the more extended radio continuum emission seen in the Brogan et al. image, the pulsar birth position lies outside of the radio remnant (see also the three color image of Brogan et al.).

Finley & Ögelman (1994) suggested that confinement by inhomogeneous, dense, star-forming gas may have shaped a complicated, asymmetric remnant, with the pulsar lying near one edge. The ambient interstellar medium, as traced by thermal $8\ \mu\text{m}$ radiation, clearly suggests an extensive interaction with the remnant. Moreover, as conjectured by Finley & Ögelman, the interstellar gas at lower Galactic longitudes probably does absorb X-ray emission from the remnant, resulting in the morphology that they reported. However, the *MSX* image shows relatively little emission at Galactic latitudes north of the pulsar position, implying less (or at least cooler) cloud material in this direction. Hence, one would naively expect the SNR to expand toward northern latitudes in addition to or instead of toward higher Galactic longitude, as seen in the 90 cm image. Although we cannot definitively rule out some pathological SNR morphology, the inferred birth position of the pulsar does not lend support to an association.

The Brogan et al. (2006) 90 cm image also shows the newly-discovered SNR G8.31–0.09 (seen in Fig. 1 as the cyan and yellow contours approximately 0.2° below the pulsar positions). The proper motion we measure rules out this remnant as the B1800–21 birth site. In addition, the range of possible birth locations do not coincide with any interesting portion of the TeV source HESS J1804–216 (Aharonian et al. 2006).

Associations between young pulsars and supernova remnants are attractive as it is widely accepted that a single supernova can produce such a pair. Some SNR / PSR associations are quite secure, such as PSR J0538+2817 and SNR S147 (Kramer et al. 2003). However, for both PSRs B1800–21 and B1757–24 the geometric coincidence and lack of contradictory data initially led to speculation of association with SNRs W30 and W28, respectively. In the case of B1757–24, a proper motion upper limit suggests insufficient velocity to allow for an association (Thorsett et al. 2002). In general, the lack of an associated radio pulsar with a known SNR is not surprising for several reasons: not all supernovae result in pulsars; not

all pulsars are oriented for favorable detection at Earth, and some pulsars are intrinsically too faint to be seen. Young pulsars without shell-type SNRs are more mysterious. The Crab nebula, created in year 1054 with PSR B0531+21, is a pulsar-powered nebula without a well-defined SNR, possibly indicating a very low energy supernova (Frail et al. 1995). The time since the supernova, the density structure of the ambient ISM, and the mass of the progenitor star greatly affect the visibility of SNRs. The lack of associations with either PSR B1800–21 or SNR W30 should not be alarming.

M. Carrillo-Barragán thanks the Academia Mexicana de Ciencias for support through its Summer of Research Program, during which the first part of this work was done. We thank D. Frail and C. Brogan for useful discussions, and C. Brogan for providing the radio-IR image of Figure 1.

REFERENCES

- Aharonian, F. et al. 2006, *ApJ*, 636, 777
- Arzoumanian, Z., Chernoff, D. F., & Cordes, J. M. 2002, *ApJ*, 568, 289
- Brand, J., & Blitz, L. 1993, *A&A*, 275, 67
- Brisken, W. F., Fruchter, A. S., Goss W. M., Herrnstein, R. S. & Thorsett, S. E. 2003, *AJ*, 126, 3090
- Brogan, C. L., Gelfand, J. D., Gaensler, B. M., Kassim, N. E., & Lazio, T. J. 2006, *ApJ*, 639, L25
- Cordes, J. M., & Lazio, T. J. W., astro-ph/0207156
- Chatterjee, S., Cordes, J. M., Lazio, T. J. W., Goss, W. M., Fomalont, E. B., & Benson, J. M. 2001, *ApJ*, 550, 287
- Clifton, T. R. & Lyne, A. G. 1986, *Nature*, 320, 43
- Faucher-Giguere, C. A., & Kaspi, V. M. 2006, *ApJ*, 643, 332
- Finley, J. P., & Ögelman, H. 1994, *ApJ*, 434, L25
- Frail, D. A., Kassim, N. E., Cornwell, T. J., & Goss, W. M. 1995, *ApJ*, 454, L129
- Frail, D. A., Kassim, N. E., & Weiler, K. W., 1994, *AJ*, 107, 1120

- Kaspi, V. M. 1996, ASP Conf. Ser. 105: IAU Colloq. 160: Pulsars: Problems and Progress, 105, 375
- Kassim, N. E., & Weiler, K. W. 1990, ApJ, 360, 184
- Kramer, M., Lyne, A. G., Hobbs, G., Löhmer, O., Carr, P., Jordan, C., & Wolszczan, A. 2003, ApJ, 593, L31
- Livingstone, M. A., Kaspi, V. M., & Gavriil, F. P. 2005, ApJ, 633, 1095
- Lockman, F. J. 1989, ApJS, 71, 469
- Manchester, R. N., Hobbs, G. B., Teoh, A. & Hobbs, M., 2005, AJ, 129, 1993
- McGary, R. S., Brisken, W. F., Fruchter, A. S., Goss, W. M., & Thorsett, S. E. 2001, AJ, 121, 1192
- Odegard, N. 1986, AJ, 92, 1372
- Thorsett, S. E., Brisken, W. F., & Goss, W. M. 2002, ApJ, 573, L111
- Zou, W. Z., Hobbs, G., Wang, N., Manchester, R. N., Wu, X. J., & Wang, H. X. 2005, MNRAS, 362, 1189

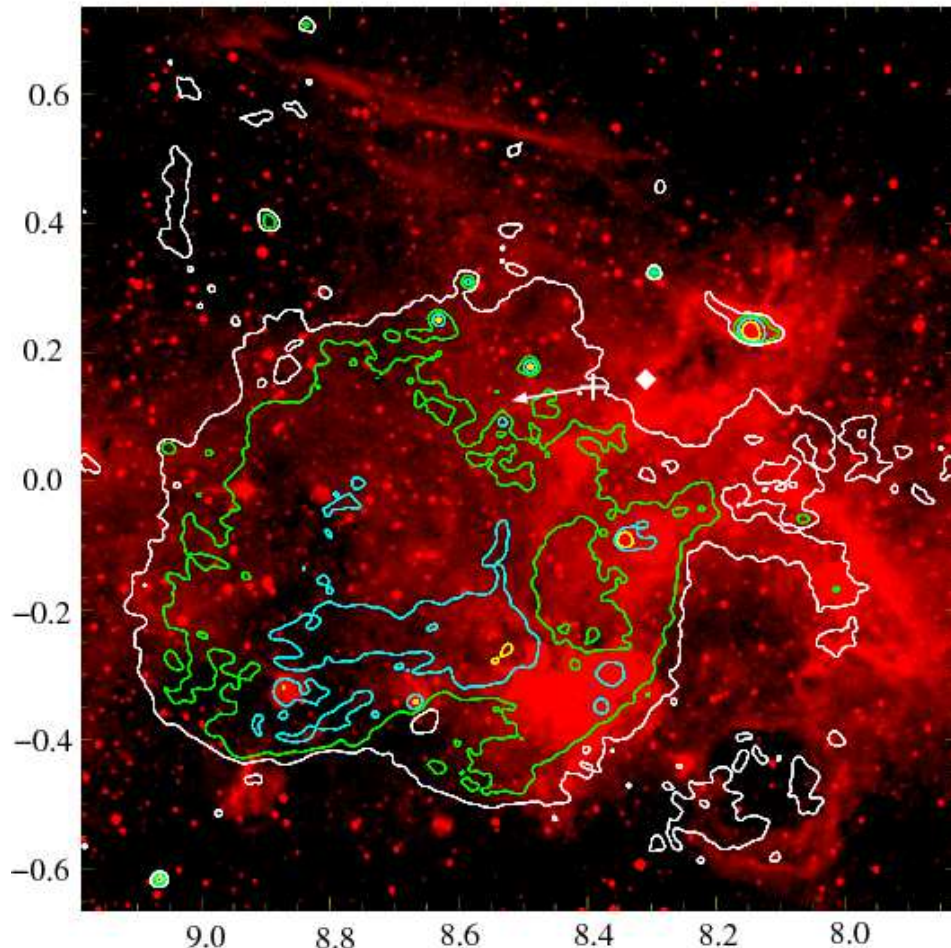


Fig. 1.— Axes are Galactic latitude (vertical) and longitude (horizontal), in decimal degrees. The red image (in logarithmic scale) shows infrared emission in the $8 \mu\text{m}$ band, as recorded by *MSX*. The contours show the 90 cm emission of the SNR; levels (in mJy beam^{-1}) are 25 (white), 50 (green), 100 (cyan), and 200 (yellow). The white contour corresponds approximately to a 5σ level. The cross shows the J2000.0 pulsar position; the diamond shows the inferred birth position (see text, §5). The arrow originating at the pulsar’s position points in the direction of its proper motion. Both correlations and anti-correlations are seen between the mid-infrared and the radio continuum emission, indicating extensive interaction between the SNR and the ambient interstellar medium.

Table 1. Observational summary

Date	Program Code	VLA Config.	λ (cm)	Synthesized Beam	Image Noise ($\mu\text{Jy beam}^{-1}$)
1993 March 14	AF244	B	3.6 [†]	$1.29'' \times 0.68'' + 2.3^\circ$	48
2005 February 5	AC774	BnA	3.6 [†]	$0.68'' \times 0.42'' - 89.0^\circ$	41
1993 January 18	AV201	A	21 [‡]	$2.05'' \times 1.08'' + 4.5^\circ$	91
2002 February 8	AC629	A	21 [‡]	$3.03'' \times 1.22'' - 28.3^\circ$	276

[†]Observations made in continuum mode.

[‡]Observations made in line mode.

Table 2. Sources in the L-band field of view

Source	R.A. (J2000)	Dec. (J2000)	θ_{sep} (arcmin)	$S_{1460\text{MHz}}^{\dagger}$ (mJy)	Comment
B1800–21	18 ^h 03 ^m 51 ^s .41	–21°37′07″.2	0	7.0	
1	18 ^h 04 ^m 38 ^s .03	–21°47′07″.6	14.8	20.5	
2 [‡]	18 ^h 04 ^m 20 ^s .42	–21°31′58″.8	8.5	12.4	3 extended components
3 [‡]	18 ^h 03 ^m 55 ^s .56	–21°31′42″.4	5.5	12.7	jet structure
4	18 ^h 03 ^m 57 ^s .71	–21°21′51″.7	15.3	10.9	point-like galaxy core
5	18 ^h 03 ^m 38 ^s .65	–21°22′37″.0	14.8	63.1	
6 [‡]	18 ^h 03 ^m 01 ^s .39	–21°48′11″.0	16.0	?	30″ size structure
7	18 ^h 02 ^m 58 ^s .91	–21°37′30″.5	12.2	13.8	
8	18 ^h 04 ^m 14 ^s .97	–21°45′42″.1	10.2	2.5	

[†]Flux densities are corrected for primary beam attenuation.

[‡]Three sources were not used as astrometry reference sources but were imaged and used in the self-calibration process.

Table 3. B1800–21 parameters

Parameter	Value
Right ascension, α (J2000)	$18^h03^m51.4105(10)^s$
Declination, δ (J2000)	$-21^\circ37'07.351(10)''$
Reference epoch (MJD)	51544
Proper motion in α , μ_α (mas yr $^{-1}$)	11.6(1.8)
Proper motion in δ , μ_δ (mas yr $^{-1}$)	14.8(2.3)
Total proper motion, μ_{total} (mas yr $^{-1}$)	$18.7_{-1.5}^{+1.4}$
Dispersion measure, DM (pc cm $^{-3}$)	233.99
NE2001 DM Distance, D (kpc)	$3.84_{-0.45}^{+0.39}$
Transverse velocity, v_\perp (km s $^{-1}$)	347_{-48}^{+57}
Pulse period, P (s)	0.13362
Pulse period derivative, \dot{P} (10^{-13})	1.3410
Characteristic age, τ_c (kyr)	15.8
Birth right ascension † , α_0 (J2000)	$18^h03^m38(2)^s$
Birth declination † , δ_0 (J2000)	$-21^\circ41'18(42)''$

† Birth location assumes τ_c accurately reflects the pulsar age.